NTHAS7: The Seventh Korea-Japan Symposium on Nuclear Thermal Hydraulics and Safety
Chuncheon, Korea, November 14- 17, 2010

Paper Number N7P0029

NUMERICAL SIMULATION OF ELECTROMAGNETIC FLOW FIELD BASED ON VECTOR FINITE VOLUME METHOD

Ryoji MURASHIGE[1], Akira YAMAGUCHI[1] and Takashi TAKATA[1]

[1] Graduate School of Engineering, Osaka University
2-1 Yamada-Oka, Suita, Osaka, Japan, 5650871
+81-6-6879-7891, murashige_r@qe.see.eng.osaka-u.ac.jp; yamaguchi@see.eng.osaka-u.ac.jp; takata_t@see.eng.osaka-u.ac.jp

ABSTRACT

The authors have developed a new numerical analysis method for electromagnetic flow field. The present method is called the Vector Finite Volume Method (VFVM) and it is based on the Vector Finite Element Method (VFEM), which automatically satisfies the solenoidal condition which means the divergence of magnetic field should be null. The VFVM has two features. One is the calculational procedure of magnetic field and the other is the arrangement of definition points of magnetic and electric field. In the VFVM, the magnetic and electric fields are placed in staggered layout and the time change rate of magnetic field is calculated from the rotation of electric field. By those operations, the VFVM does not need the iterative procedure for the solenoidal condition. However, a consideration of boundary condition of electric field will be required in the VFVM. In the present study, the authors have proposed a new method of giving boundary electric field and analyzed some benchmark analyses in order to estimate its applicability. It is concluded the new method is applicable in the VFVM.

1. INTRODUCTION

Liquid sodium used for a coolant of fast reactor is electromagnetic fluid. In the electromagnetic fluid, the Lorentz force is generated by the interaction of a magnetic field and an induced electric field. Since the velocity field is influenced by the Lorentz force, it comes to be possible that a flow structure is intentionally adjusted by controlling the Lorentz force or the magnetic field. From this viewpoint, it is meaningful to depict the behavior of electromagnetic flow under an applied magnetic field. A numerical simulation is useful for investigating the fluid dynamics characteristics under an electromagnetic field.

In the numerical simulation of the electromagnetic fluid, emphasis should be placed on solving the induction equation consistent with the solenoidal condition. The solenoidal condition requires that the divergence of magnetic field should be null at any point in space. This condition is a prerequisite in a physical consistency viewpoint. However, in the discretized fundamental equations, the solenoidal condition may not be always strictly satisfied. In addition, in the induction equation, the solenoidal condition is not the sufficient condition but a necessary condition. Hence a numerical technique needs to be developed in order to satisfy the solenoidal condition when we solve the induction equation in a numerical manner. In precedent works, iterative procedure techniques have been adopted (Oki *et al.*, 1992, 1995, Nakai *et al.*, 1997), but it causes an increase of the computational cost in general. For improving the computational efficiency, it is desirable to solve the induction equation without iterative method or with a less number of iterations.

The Vector Finite Element Method is the numerical method that is able to solve the equations without iterations (Matsumoto *et al.*, 2003). We apply this methodology to the finite volume method (called the Vector Finite Volume Method, VFVM). The VFEM is based on a finite element method and it is necessary to solve a matrix to obtain the primitive variables, which results in a significant computing cost for large scale problems. Therefore, the VFVM has an advantage in terms of the computational cost compared with the VFEM. However, a special consideration of electric field at boundary is required suitable for the VFVM.

In this paper, we have proposed a new method that can treat the boundary condition appropriately and carried out benchmark analyses. A parallel plate flow under applied magnetic field (Hartman flow) is analyzed firstly. The computational results are compared with the theoretical solution and another numerical results by Oki *et al.* (1992). A three dimensional rectangular channel flow with a magnetic field is also analyzed.

2. NUMERICAL MODEL

2.1 Governing Equations

The governing equations of electromagnetic fluid include a coupling terms of velocity field and magnetic field. In the present work, the following assumptions are adopted:

(a) material properties are constant
(b) temperature field is fixed
(c) gravity force is neglected
(d) negligible displacement current, convection current and coulomb force.

With those assumptions, the governing equations are simplified as follows:

$$\nabla \cdot \mathbf{u} = 0 , \tag{1}$$

$$\frac{\partial \mathbf{u}}{\partial t} + \mathbf{u} \cdot \nabla \mathbf{u} = -\frac{1}{\rho} \nabla p + \nu \nabla^2 \mathbf{u} + \frac{1}{\rho} \mathbf{f}_L , \tag{2}$$

$$\nabla \cdot \mathbf{B} = 0 , \tag{3}$$

$$\frac{\partial \mathbf{B}}{\partial t} = \nabla \times (\mathbf{u} \times \mathbf{B}) - \frac{1}{\sigma \mu} \nabla^2 \mathbf{B} . \tag{4}$$

Here, $\mathbf{u}$, t, p, $\mathbf{f}_L$ and $\mathbf{B}$ mean the velocity field, time, pressure, Lorentz force and magnetic flux density, respectively. ρ, ν, σ and μ are the density, kinetic viscosity, electric conductivity and magnetic permeability, respectively.

Equations (1) and (2) are the governing equations of fluid dynamics. In the numerical simulation, these equations are solved with Simplified Marker and Cell (SMAC) method.

$\mathbf{f}_L$ in Eq. (2) is the Lorentz force. It is the coupling term between flow and electromagnetic fields. It is obtained in the following equation.

$$\mathbf{f}_L = (\frac{1}{\mu} \nabla \times \mathbf{B}) \times \mathbf{B} . \tag{5}$$

Electromagnetic field is described by Eqs. (3) and (4). Equation (4) is called induction equation that is derived by coupling of the Ohm's law and the Maxwell equations of electromagnetism and we need to solve it consistent with Eq. (3), which means the divergence of magnetic field should be zero (*i.e.*, solenoidal condition). Oki *et al.* (1992) applied B method to achieve this problem. The B method employs iterative procedure in the induction equation. However it causes an increase of computation time.

In order to avoid the iterations, Matsumoto (2003) developed VFEM based on a finite element method. In the VFEM, Eq. (4) is divided into two equations and the electric field is defined at the sides of the cell surface. We have extended this methodology to a finite volume method.

2.2 Vector Finite Volume Method

In the VFVM, Eq. (4) is separated into the following equations:

$$\mathbf{E} = -\mathbf{u} \times \mathbf{B} + \frac{1}{\sigma \mu} \nabla \times \mathbf{B} , \tag{6}$$

$$\frac{\partial \mathbf{B}}{\partial t} = -\nabla \times \mathbf{E} . \tag{7}$$

Above the equations, $\mathbf{E}$ is the electric field. Here, let us consider the solenoidal condition. Adding the divergence operation of Eq. (7), one obtains Eq. (8).

$$\frac{\partial}{\partial t} (\nabla \cdot \mathbf{B}) = -\nabla \cdot (\nabla \times \mathbf{E}) = 0 . \tag{8}$$

The divergence of the rotation operation vanishes mathematically. In the VFVM, the arrangement of variables in electromagnetic field is given so as to satisfy Eq. (8) not only mathematically, but also computationally. Figure 1 shows the arrangement of variables in the electromagnetic field. The magnetic flux density is defined at the center of the cell surface, while electric field is given at each side of the cell.

The concept of the VFVM is shown in Fig. 2. According to Stokes' theorem, the surface integral of $\nabla \times \mathbf{E}$ is equivalent to the line integral of the electric field along with the boundary surface sides. In terms of S_1 and S_2, the direction of the line integral of $\mathbf{E}$ on the line l is reversed. Therefore the value of line integral at line l is cancelled out. Considering at all surfaces in one control volume, the value of any line integral of $\mathbf{E}$ is canceled. Consequently, the divergence of $\nabla \times \mathbf{E}$ becomes zero definitely, which means the proposed computational procedure assures that Eq. (8) is unconditionally satisfied.

Since time variation of $\nabla \cdot \mathbf{B}$ is zero, Eq. (8) is rewritten as:

$$\nabla \cdot \mathbf{B}^{n+1} = \nabla \cdot \mathbf{B}^{n} = .. = \nabla \cdot \mathbf{B}^{0} , \tag{9}$$

where, superscripts n+1, n and 0 mean the next, current and initial time step respectively. Accordingly, when the solenoidal condition is achieved at the initial condition, it is satisfied automatically at all the times step that follow. Thus, no iteration for the solenoidal condition is required in the VFVM, which is a great advantage from the viewpoint of the computational efficiency.

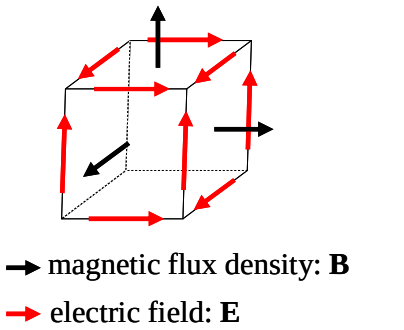

Fig. 1 Arrangement of E and B in VFVM

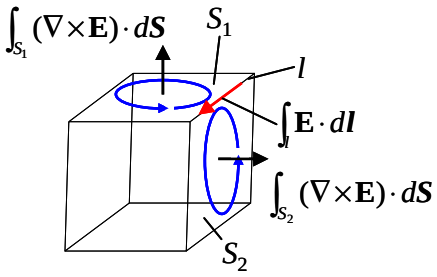

Fig. 2 Conceptual diagram of VFVM

2.3 Boundary Condition of Electric Field

The VFVM is based on a finite volume method, and does not require the iterative procedure for $\nabla\cdot\mathbf{B}=0$. Hence it is expected that less computation time is needed in the VFVM comparing with the B method.

However, we should consider the appropriate electric field at the boundary in the VFVM. It is noted that the boundary condition of electric field is included in the discretized equation in the VFEM. So no consideration of boundary **E** is necessary. On the other hand, VFVM is not included the boundary condition of **E** when the governing equation is discretized. Hence it is necessary to give the boundary electric field as boundary condition.

Some problems will occur if no consistency between electric field and magnetic flux density is applied. Let us consider a concrete example. If the constant magnetic flux density is embedded at boundary, the boundary condition of **E** is:

$$\left.\frac{\partial\mathbf{B}}{\partial t}\right|_{boundary} = -(\nabla\times\mathbf{E})\big|_{boundary} = 0 \qquad (10)$$

If the boundary electric field is zero, Eq. (10) is valid (in this paper, we say it "E_b=0"). However, it results in the inconsistency between boundary condition of **E** and **B** because zero electric field does not always satisfy Eq. (6). As a result, unrealistic magnetic flux density could be calculated.

Additionally, the conformation of the actual boundary surface and the computational cell surface is also of importance. It is also noted that the consideration of the electric field comes from the boundary condition of magnetic flux density given in the numerical simulation rather than the material characteristics at boundary.

In the present study, the authors have proposed a new method for defining the boundary condition of electric field in the computational procedure.

2.4 Proposal of New Method

The electric field at the side of the boundary surface is evaluated using a corrector. Figure 3 shows the concept of the corrector of the electric field at the boundary in the proposed method. The corrector δe, is defined at each cell (in this paper, we call it "cell-corrector"). And the difference of two contiguous δe (δe_{left}, δe_{right}, in Fig. 3) is designated as "edge-corrector (δE_b)". In the proposed method, the boundary electric field is expressed as a sum of a predictor and an "edge-corrector" (see Eq. (11) and Fig. (3)).

$$\begin{aligned} E_b &= E_b^* + \delta E_b \\ &= E_b^* + (\delta e_{left} - \delta e_{right}) \end{aligned} . \qquad (11)$$

Here, E_b^* is the predictor and is obtained by the following equation:

$$\mathbf{E}_b^* = \left(-\mathbf{u}\times\mathbf{B} + \frac{1}{\sigma\mu}\nabla\times\mathbf{B}\right)\Big|_{boundary} . \qquad (12)$$

That is to say, Equation (6) is used for the calculation of **E** in the computational cell and the boundary predictor.

By substituting Eq. (11) into the boundary condition of the electric field (Eq. (10), for instance), one obtains a system of equations. In the present study, Bi-Conjugate Gradient Stabilized (BiCGS) method is applied for the matrix solver.

The present method corrects the boundary **E** only at the boundary surfaces, while the iterative procedure method performs the correction of the magnetic field at all computational cells, including inner cells. Hence the present method has an advantage to enhance the computational efficiency as the matrix size increases. It is said that the corrector behaves as if it is an external force that keeps the magnetic flux density constant on the boundary.

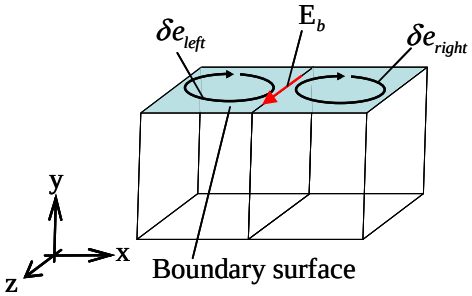

Fig. 3 Method for giving corrector of boundary electric field

2.5 Computational Method

In the present study, a finite difference with a structural mesh arrangement in Cartesian coordinates is applied. With regard to the differential scheme, a second order central difference is applied in a diffusion term, and a first order upwind difference scheme is used in a convection term. With regard to the electromagnetic fields, the Lorentz force $\mathbf{f}_L$, Eqs. (6) and (7) are discretized explicitly. The flow chart of the calculation procedure is shown in Fig. 4

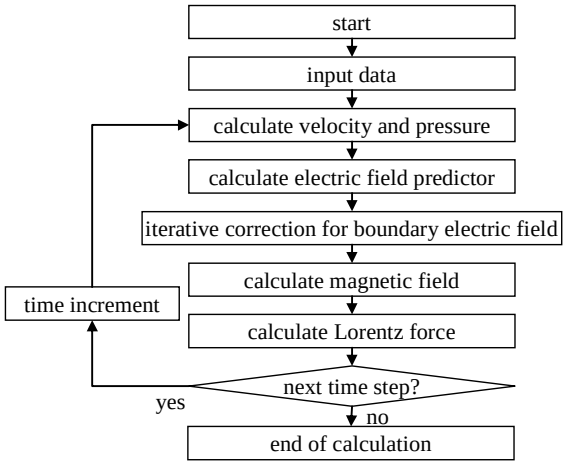

Fig. 4 Flow chart of calculation

3. BENCHMARK ANALYSES

3.1 Parallel Plate Flow with Magnetic Field

In order to investigate the applicability of the proposed method, we analyze a parallel plate flow under an applied magnetic field. This flow is called the Hartmann flow. We compare the analytical result of the VFVM to that of the B method (Oki, *et al.*,1992).

3.1.1 Analytical conditions

The analytical model is shown in Fig. 5. The size of the analytical region is 20(x)×2.0(y)×2.5(z)[m]. Inlet velocity is given as the parabolic distribution with 1.0[m/s] average velocity. The outlet boundary condition is constant pressure (P_B=0[Pa]). A non-slip condition is given on the parallel plates wall (y=0, 2.0[m]) and a free-slip condition is applied in the span direction. With regard to a boundary condition of the magnetic field, a constant magnetic flux density (B_y=1.0[T]) is embedded in vertical direction on the parallel plate each (y=0, 2.0[m]). In order to achieve the solenoidal condition, the initial condition of the magnetic flux density is uniform (**B**=(0.0, 1.0, 0.0)) in whole analytical region.

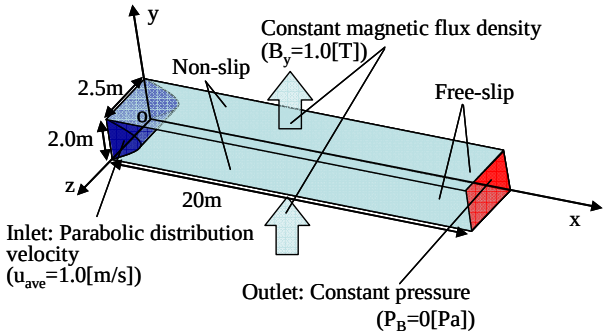

Fig. 5 Hartmann flow analytical region

The computational domains are divided into 16(x)×20(y)×2(z) of an equal cell sizes. The time increment (Δt) and calculation time (t_{end}) are set to 1.0×10^{-4}[s] and 2.0[s], respectively. The convergence criteria of pressure and electric field equations are both 1.0×10^{-8}. Working fluid is a virtual one and its properties are shown in Table 1. The conditions are determined based on Oki's numerical experiment using B method (1992) so that one can make a comparison.

In the Hartmann flow analysis, the boundary condition of magnetic flux density is given as constant in the parallel plates. As mentioned in Sec. **2.3**, the condition needs the satisfaction of Eq. (10). Hence the boundary condition of electric field is $-(\nabla\times\mathbf{E})\big|_{boundary}=0$. Previously, we defined the boundary electric field as null ("Eb=0" assumption) in order to achieve the condition. However, if we employ the assumption in VFVM, the magnetic flux density profile differs from that of B method as mentioned later. We apply the proposed methodology for more accurate estimation using the VFVM.

Table1. Fluid properties (parallel plate flow)

Property	Density [kg/m^3]	Kinetic viscosity [m^2/s]	Electric conductivity [S/m]	Magnetic permeability [H/m]
Value	1.0	0.1	0.16	6.25

3.1.2 Results and discussions

Figure 6 shows the cross sectional distributions of (a) the velocity and (b) the Lorentz force vectors. The Lorentz force near wall directs to the positive direction, which accelerate the fluid flow. On the other hand, it turns toward the negative direction in the center part. Hence, the axial velocity profile tends to flatten according the Lorentz force.

In order to evaluate the applicability of the proposed method, the analytical results are compared with the theoretical solution. The theoretical velocity profile of Hartmann flow is obtained as the following equation.

$$u(y)=\frac{Ha}{\tanh(Ha)\text{-}Ha}\left\{\frac{\cosh(Ha*y)}{\cosh(Ha)}-1\right\}. \quad (13)$$

Here, u is the velocity in the main flow direction and *Ha*

is the Hartmann number and it is defined as:

$$Ha=\sqrt{\frac{\sigma}{\rho\nu}}B_0L\,, \qquad (14)$$

where, B_0 is the magnitude of the applied magnetic flux density and L is the half distance between two parallel plates. Equation (14) indicates the Hartmann number is a dimensionless number that represents the relative importance of the electromagnetic force and the viscous force. In this case, *Ha* is 4.0.

The comparisons of the velocity profiles and the magnetic flux density profiles at x=15.0[m] are shown in Fig. 7 (a) and (b). We can see that the velocity profiles calculated by the present method ("Present") and based on the "Eb=0" assumption agree well with the theoretical results.

However, as seen in Fig.7 (b), the magnetic flux density profile of "E_b =0" assumption is different from "B method". This is attributed to the difference in the treatment of the boundary electric field. In other words, a larger magnetic flux density is calculated near boundary because E_b=0 brings a large gradient of electric field. On the other hand, since the boundary electric field is corrected in the "Present" case, such inconsistency does not appear. It is noted that the "Present" case is in good agreement with the "B method" case.

Figure 7 (c) shows the comparison of Lorentz force in x direction between "Present" and "E_b =0" cases. It is noted that the Lorentz force profile of the "Present" case has a similar shape with some parallel shift on the "E_b =0" case. Therefore, a similar velocity profile is obtained in spite of the difference in the magnetic flux density profile. In other words, the velocity profile is determined based on not the magnitude of Lorentz force, but the shape of that profile. Instead, the difference of the magnitude of the force leads the different pressure gradient as seen in Fig. 8. Figure 8 shows the comparison of pressure contours between "Present" and "E_b=0" cases. High pressure gradient is seen in the "E_b=0" case, which means an incorrect electric field leads inaccurate results. Hence, it is essential to consider the boundary electric field for accurate estimation of the magnetic fluid flow performance.

The present results indicate that the proposed method can deal with the boundary electric field successfully with a reasonable and practical computing time.

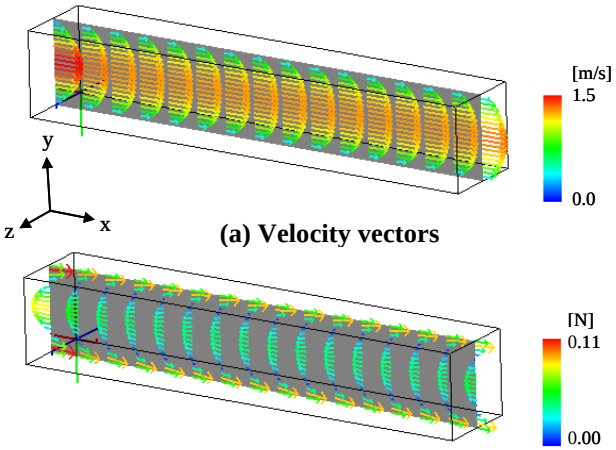

(a) Velocity vectors

(b) Lorentz force vectors

Fig. 6 Analytical results of Hartman flow (Present method)

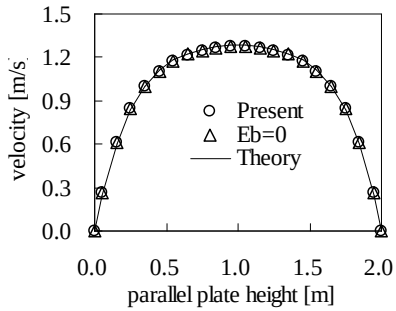

(a) Velocity profiles

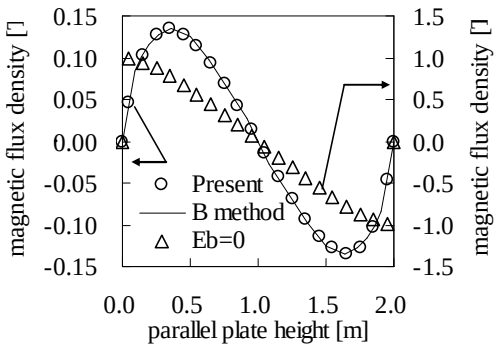

(b) Magnetic flux density profiles

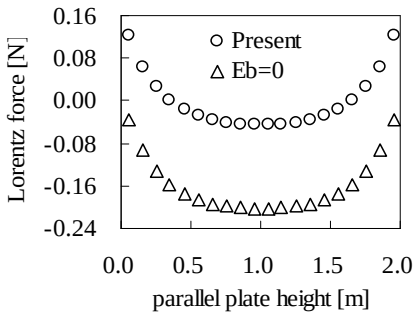

(c) Lorentz force profiles

Fig. 7 Comparison of profiles at x=15.0m

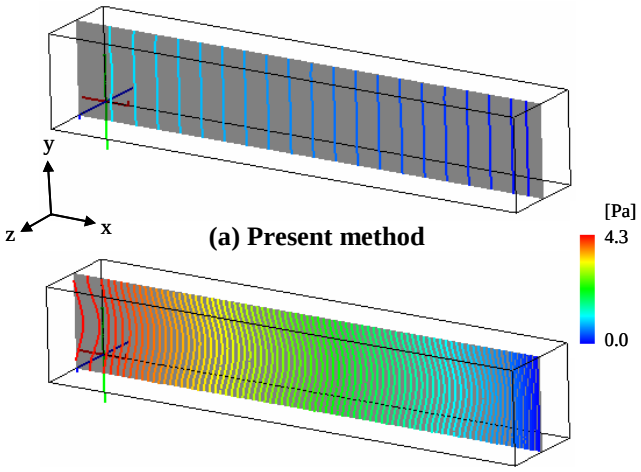

(a) Present method

(b) E_b=0

Fig. 8 Comparison of iso-pressure contours (Δp=0.05)

3.2 Rectangular Channel Flow Analysis

3.2.1 Analytical conditions

Figure 9 shows the analytical region of a rectangular channel flow. The size of the region is 10(x)×2.0(y)×2.0(z)[m]. The non-slip condition is applied both in the x-y plane at z=0, 2.0[m] and in the x-z plane at y=0, 2.0[m]. Fully developed flow velocity is given in the inlet, and the outlet pressure is given as a constant value (P_B=0[Pa]). In the analytical region, a constant magnetic flux density is applied only from x=3.0 to 6.5[m] (blue region in Fig. 9). In this paper, the region is called "magnetic region". In the other region, no magnetic flux is applied (**B**=0[T]).

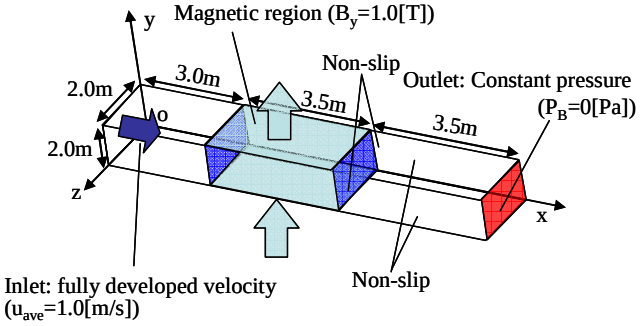

Fig. 9 Analytical region of rectangular channel flow

The computational region is segmented into 20(x)×20(y)×20(z) equally. The properties of the working fluid are shown in Table 2. In order to exaggerate the effect of electromagnetic field, larger *Ha* number (*Ha*=10.0) is assumed than in Sec. **3.1**. The time step(Δt) is set to 2.0×10^{-4}[s] in order to satisfy the Courant-Friendrichs-Lewy (CFL) number <0.1. Simulation is conducted until a steady state is achieved.

Table2. Fluid properties (rectangular channel flow)

Property	Density [kg/m^3]	Kinetic viscosity [m^2/s]	Electric conductivity [S/m]	Magnetic permeability [H/m]
Value	0.1	0.1	1.0	1.0

3.2.2 Results and discussions

Figure 10 shows the cross sectional velocity vectors at the center of the duct. Fluid is deaccelerated in the magnetic region (blue region in Fig. 10). In the downstream of the magnetic region, the fluid recovers the parabolic distribution velocity.

Pressure contour is shown in Fig. 11. In the Hartmann flow (see Sec. **3.1**), there is no pressure gradient in y direction in the present method. On the contrary, a multi-dimensional pressure gradient arises in the rectangular channel flow. This indicates that an applied magnetic field conduces to a multi dimensional effect.

Pressure change in x-z plane from the inlet to the outlet of the duct is illustrated in Fig. 12. As seen in Fig. 12, the pressure increases at the entrance of magnetic region once. Then, the pressure decreases rapidly in the magnetic region. After the magnetic region, pressure gradient becomes a slow gradual change. Those tendencies agree well with Kumamaru's numerical experiment (2004).

In the present study, we have performed two types of analyses in terms of computational mesh in corrected surface. One is the square (*i.e.*, Δx:Δz=1:1, Sec **3.1**) and the other is the rectangular (Δx:Δz=5:1, Sec. **3.2**) (See Fig. 13). Here, Δx and Δz is the length of one computational mesh in x direction and z direction, respectively. Since we have obtained good results in both analyses, the proposed method has robustness in respect to the aspect ratio of mesh arrangement. Therefore, it is concluded that the proposed method has applicability in terms of computational mesh.

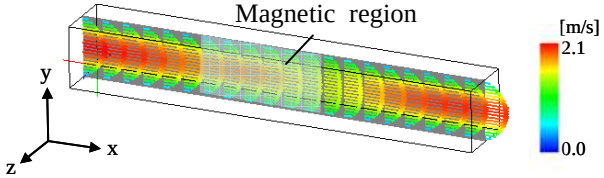

Fig. 10 Velocity vectors of rectangular channel flow

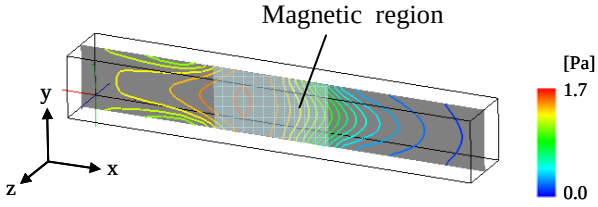

Fig. 11 Pressure contour (Δp=0.1)

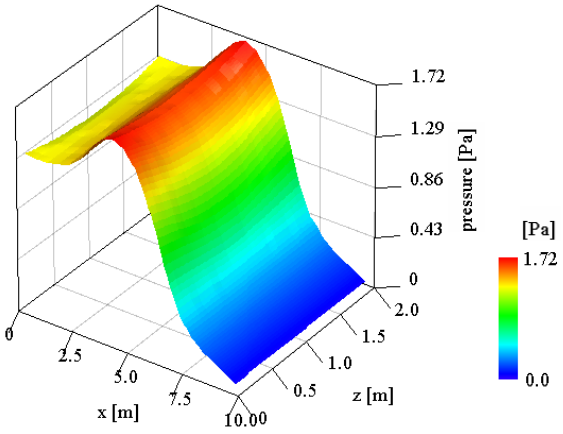

Fig. 12 Pressure change in x-z plane at y=1.0[m]

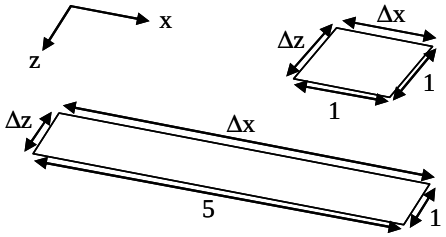

Fig.13 Aspect ratio of mesh in corrected surface

4. CONCLUSIONS

In the present paper, the authors have extended the concept of the Vector Finite Element Method to a finite volume method which is named the Vector Finite Volume Method (VFVM). Then, a new method for giving boundary electric field is proposed. From the benchmark analysis, the following conclusions are obtained.

In the case of boundary electric field set to zero ("E_b =0" case), a large magnetic flux density is generated. It is due to the physical inconsistency between **E** and **B** at the boundary induced by numerical algorithm. As a result, magnetic flux density profiles of "E_b =0" case is different from that of "B method" case. In addition, a large pressure gradient arises in that case. From those results, it is confirmed that the consideration of boundary electric field is needed.

In the present method, both velocity profile and magnetic flux density profile are in good agreement with the theoretical or other numerical results. Hence the proposed method is considered as available technique for the VFVM.

The proposed method corrects the electric field only at boundary surfaces, while other numerical techniques such as solving the induction equation iteratively perform the iteration for all computational cells. So the matrix size of a system of equations becomes smaller. Consequently, a lower computational cost is achieved.

From the result of the present analyses, the aspect ratio of computational mesh in corrected surface has no influence on the proposed correction method. Hence, the new method has wide adaptive flexibility in the computational mesh selection.

NOMENCLATURE

B	magnetic flux density vector	[T]
E	electric field vector	[V/m]
E_b	electric field vector at boundary	[V/m]
E_b^*	boundary electric field predictor	[V/m]
δE	"edge-corrector" of boundary electric field	[V/m]
δe	"cell-corrector" of boundary electric field	[V/m]
$\mathbf{f}_L$	Lorentz force vector	[N]
Ha	Hartmann number	[-]
p	pressure	[Pa]
t	time	[s]
t_{end}	calculation time	[s]
Δt	time increment in computation	[s]
u	velocity vector	[m/s]

Greek Letters

μ	magnetic permeability	[H/m]
ν	kinetic viscosity	[Pa s]
ρ	density	[kg/m^3]
σ	electric conductivity	[S/m]

Superscripts

n	present time step
n+1	next time step
0	initial time step

REFERENCES

Oki, Y *et al.* (1995). "Numerical Analysis of Natural Convection of Thermoelectrically Conducting Fluids in a Square Cavity under a Uniform Magnetic Field," *JSME International Journal*, Series B, Vol. 38, No.3 pp.374-381

Matsumoto, M *et al.* (2003). "Numerical Analysis of Thermo-electrically Conducting Fluids in a Cubic Cavity Using Vector Finite Element Method for Induction Equations," *ISIJ International*, Vol. 43, No.6 pp.932-941

Takata, T *et al.* (2010). "Numerical Study on Passive Control of Thermal Striping Phenomenon Using Lorentz Force in Fast Reactor," *Proc. of ICONE 18*, ICONE18-30188, Xi'an, China.

Kumamaru, H *et al.* (2004). "Three-Dimensional Numerical Calculations on Liquid-Metal Magnetohydrodynamic Flow in Magnetic Field Inlet-Region," *Journal of NUCLEAR SCIENCE and TECHNOLOGY*, Vol.41, No.5, pp.624-631

Oki, Y *et al.* (1992). "Entrance Flows of Electrically Conducting Fluids between Two Parallel Plates," *JSME, B*, 58-545 pp.14-21 [in Japanese]

Nakai, T *et al.* (1997). "Numerical Analysis of Natural Convection in Thermoelectrically Conducting Fluids in a Cubic Cavity under a Constant Magnetic Field (2nd report)," *JSME, B,* 63-605 pp.201-208 [in Japanese]